Available online at www.pelagiaresearchlibrary.com

Pelagia Research Library

Advances in Applied Science Research, 2012, 3 (1):60-74

Pelagia Research Library

ISSN: 0976-8610
CODEN (USA): AASRFC

Thermophoresis and viscous dissipation effects on Darcy–Forchheimer MHD mixed convection in a fluid saturated porous media

N. Kishan[1] and Srinivas Maripala[2]

[1]*Department of Mathematics, University College of Science, Osmania University, Hyderabad, A.P., India*
[2]*Department of Sciences and Humanities, Sreenidhi Institute of science and Technology, Yamnampet, Ghatkesar, Rangareddy, A.P., India*

ABSTRACT

An analysis is presented to investigate the effects of thermophoresis on MHD Mixed convection, heat, and mass transfer about an isothermal vertical flat plate embedded in a fluid-saturated porous medium in the presence of viscous dissipation . The similarity solution is used to transform the problem under consideration into a boundary value problem of coupled ordinary differential equations, which are solved numerically by using the finite difference method. Numerical computations are carried out for the non-dimensional physical parameter. The results are analyzed for the effect of different physical parameters such as thermophoretic , MHD, mixed convection, Eckert number, inertia parameter, buoyancy ratio, and Schmid number on the flow, heat, and mass transfer characteristics.

Keywords: MHD, Viscous dissipation, Porous media, Mixed convection, Thermophoresis, Finite difference method.

INTRODUCTION

Natural convective flow and heat transfer in saturated porous media is gaining more attention because of its wide applicability in packed beds, porous insulation, beds of fossil fuels, nuclear waste disposal, resin transfer modeling, etc. Over the past two decades, studies in aerosol particle deposition due to thermophoresis have gained importance for engineering applications. The technological problems include particle deposition onto wafers in the microelectronics industry, particle surfaces produced by condensing vapor–gas mixtures, particles impacting the blade surface of gas turbines, and others such as filtration in gas cleaning and nuclear reactor safety. In engineering particle, usually more than one mechanism can act simultaneously and their interactions need to be considered for accurate prediction of deposition rates. In this work, the mechanism of particle deposition onto a vertical surface by the coupled effects of viscous dissipation, mixed convection, and thermophoresis is examined.

Most of the research efforts [1], [2], [3] and [4] concerned free convection using Darcy's law, which states the volume-averaged velocity is proportional to the pressure gradient. The Darcy model is shown to be valid under conditions of low velocities and small porosity. In many practical situations, the porous medium is bounded by an impermeable wall, has high flow rates, and reveals non uniform porosity distribution in the near-wall region, thereby making Darcy's law inapplicable. To model the real physical situations better, it is therefore necessary to include the non-Darcian effects in the analysis of convective transport in a porous medium.

Small particles, such as dust, when suspended in a gaseous medium possessing a temperature gradient, it will move inthe direction opposite to the temperature gradient. This motion is known as thermophoresis, occurs because gas

molecules colliding on one side of a particle have different average velocities from those on the other side due tothe temperature gradient. This phenomenon has been the subject of considerable study in the past. In optical fiber synthesis, thermophoresis has been identified as the principal mechanism of mass transfer as used in the technique of modified chemical vapor deposition (MCVD) [5]. Thermophoresisa gaseous mixture of re active precursors is directed over a heated substrate where solid film deposits are located. In particular, the mathematical modeling of the deposition of silicon thin films using MCVD methods has been accelerated by the quality control measures enforced by the micro-electronics industry. Such topics involve a variety of complex fluid dynamical processes including thermophoretic transport of particles deposits, heterogenous/homogenous chemical reactions, homogenous particulate nucleation and coupled heat and energy transfer.

The problem of Darcy–Forchheimer mixed convection heat and mass transfer in fluid-saturated porous media was studied by Rami et al. [6]. Goren [7] was one of the first to study the role of thermophoresis in the laminar flow of a viscous and incompressible fluid. He used the classical problem of flow over a flat plate to calculate deposition rates and showed that substantial changes in surface deposition can be obtained by increasing the difference between the surface and free stream temperatures. This was later followed by the effect of thermophoresis on particle deposition from a mixed convection flow onto a vertical plate by Chang et al. [8] and Jayaraj et al. [9]. Also, Tsai [10] obtained the effect of wall suction and thermophoresis on aerosol particle deposition from a laminar flow over a flat plate. Selim et al. [11] discussed the effect of surface mass transfer on mixed-convection flow past a heated vertical permeable flat plate with thermophoresis. Chamkha and Pop [12] studied the effect of thermophoretic particle deposition in free convection boundary layer from a vertical flat plate embedded in a porous medium. Peev et al. [13] discussed the problem of heat transfer from solid particles to power low non-Newtonian fluid in a granular bed at low Reynolds number.

Most previous studies of the same problem neglected viscous dissipation and thermophoresis. But Gebhart [14] has shown that the viscous dissipation effect plays an important role in natural convection in various devices that are subjected to large variations of gravitational force or that operate at high rotational speeds. Motivated by the above investigations and possible applications.

Hence,in this paper we aim at analyizing the influence of MHD on mixed convection flow , heat and mass transfer about an isothermal vertical plate embedded ina fluid saturated porous medium and the effects of viscous dissipation and thermophoresis in both aiding and opposing flows. Thermophoresis is also a key mechanism of study in semi-conductor technology,especially controlled high-quality wafer production aswell as in radioactive particle deposition in nuclear reactorsafety simulations and MHD energy generation system operations. A number of analytical and experimental papers in thermophoretic heat and mass transfer have been communicated. Talbot et al. [17] presented a seminal study, considering boundary layer flow with thermophoretic effects, which has become a benchmark for subsequent studies. The thermophoretic flow of larger diameter particles was investigated by Kanki et al. [18]. Recently, M.A.Seddek [19], studied the influence of viscousndissipation and thermophoressis in Darcy- forcheimer mixed convection heat and mass transfer in fluid –saturated porous media.

Mathematical formulation

Consider the steady mixed convection boundary layer over a vertical flat plate of constant temperature T_w and concentration C_w , which is embedded in a fluid-saturated porous medium of ambient temperature T_∞ and concentration C_∞ , respectively. The x-coordinate is measured along the plate from its leading edge and the y-coordinate normal to it. Allowing for both Brownian motion of particles and thermophoretic transport, the governing boundary layer equations are

$$\frac{\partial u}{\partial x}+\frac{\partial v}{\partial y}=0 \tag{1}$$

$$[1+\frac{\sigma B_0^2 K}{\rho \nu}]\frac{\partial u}{\partial y}+\frac{c_f\sqrt{K_1}}{\nu}\frac{\partial u^2}{\partial y}=\mp g\left(\frac{K_1}{\nu}\right)\ [\beta_T\frac{\partial T}{\partial y}+\beta_C\frac{\partial C}{\partial y}] \tag{2}$$

$$u\frac{\partial T}{\partial x}+v\frac{\partial T}{\partial y}=\frac{\lambda g}{\rho c_p}\frac{\partial^2 T}{\partial y^2}+\frac{\nu}{c_p}\ (\frac{\partial u}{\partial y})^2 \tag{3}$$

$$u\frac{\partial C}{\partial x}+v\frac{\partial C}{\partial y}=D\frac{\partial^2 C}{\partial y^2}-\frac{\partial}{\partial y}(V_T C) \tag{4}$$

The boundary conditions are given by

y=0, v = 0, T =T_w , C= C_w ,
y →∞, u= u_∞ , T= T_∞, C= C_∞ , (5)

where u, v are velocity components along x,y coordinates, respectively, T and C are, respectively, the temperature and concentration, cf is the Forchheimer coefficient, K_1 is the Darcy permeability, g is the acceleration due to gravity, v is the kinematic viscosity, β_T is the coefficient of thermal expansion, β_C is the coefficient of concentration expansion, C_p is the specific heat of the fluid at constant pressure, q_r is the radiative heat flux, and D is the mass diffusivity. In Eq. (2), the plus sign corresponds to the case where the buoyancy force has a component "aiding" the forced flow and the minus signs refer to the "opposing" case.

In Eq. (4), the thermophoretic velocity V_T was given by [16]

$$V_T = - k\, v \frac{\Delta T}{T} = - \frac{k\, v}{T} \frac{\partial T}{\partial y}, \quad (6)$$

where k is the thermophoretic coefficient, which is given by [17] as

$$k = \frac{2C_s(\lambda_g/\lambda_p + C_t K_n) C_1}{(1+3C_m K_n)(1+2\lambda_g/\lambda_p + 2C_t K_n)} \quad (7)$$

Where C_m, C_s, and C_t are constants and λ_g and λ_p are the thermal conductivities of the fluid and diffused particles, respectively. C_1 is the Cunningham correction factor and K_n is the Knudsen number.

Now we define the following dimensionless variables for mixed convection

$$\eta = \frac{y}{x} Pe_x^{1/2}, \qquad \psi = \alpha\, Pe_x^{1/2} f(\eta),$$
$$\theta(\eta) = \frac{T - T_\infty}{T_w - T_\infty}, \qquad \varphi(\eta) = \frac{C - C_w}{C_w - C_\infty}, \quad (8)$$

where ψ is the stream function that satisfies the continuity equation and η is the dimensionless similarity variable. With these changes of variables, Eq. (1) is identically satisfied and Eqs. (2), (3) and (4) are transformed to

$$(1+Ha^2) f'' + 2\Lambda f' f'' = \mp \left(\frac{Ra_x}{Pe_x}\right)(\theta' + N\varphi'), \quad (9)$$

$$\theta'' + \frac{1}{2} f \theta' + Pr\, Ec\, (f'')^2 = 0, \quad (10)$$

$$\frac{1}{Sc}\varphi'' - \tau(\varphi\theta'' + \theta'\varphi') + \frac{1}{2Pr} f \varphi' = 0 \quad (11)$$

The corresponding boundary conditions take the form

$$f(0)=0, \quad \theta(0)=1, \quad \varphi(0)=1$$
$$f'(\infty)=1, \quad \theta(\infty)=0, \quad \varphi(\infty)=0 \quad (12)$$

where the primes denote differentiation with respect to η,

$\Lambda = C_f \sqrt{K_1}\, u_\infty / v$ is the inertia parameter,

$Ra_x = (K_1 g \beta_T)\left(\frac{(T_w - T_\infty)x}{\alpha v}\right)$ is the thermal Rayleigh number,

$Pe_x = \frac{u_\infty x}{\alpha}$ is the local Peclet number,

$N = \frac{\beta_C(C_w - C_\infty)}{\beta_T(T_w - T_\infty)}$ is the buoyancy ratio,

$\tau = -K \frac{(T_w - T_\infty)}{T}$ is the thermophoretic parameter, and

$Ec = u_\infty^2 / C_P(T_w - T_\infty)$ is the Eckert number.

The important physical quantities of our interest are the Nusselt number Nu_x and Sherwood number Sh_x . These can be defined as follows:

$Nu_x = (\frac{q_w x}{(T_w - T_\infty)k}) = -1/2\ Pe_x^{1/2}\theta'(0)$,

$q_w = -k\,(\frac{\partial T}{\partial y})\ y=0$ (13)

$Sh_x = (\frac{J_w x}{(C_w - C_\infty)D}) = -\ Pe_x^{1/2}\varphi'(0)$,

$J_w = -D\,(\frac{\partial C}{\partial y})\ y=0$ (14)

The system of equations (9),(10) and (11) are coupled and nonlinear Ordinary Differential Equations. First the equation (9) is liberalized by using the Quasi-linearization technique Bellman,kalaba we obtain

$(1+Ha^2+2\Lambda F')f'' + (2\Lambda F'')f' = \mp(\frac{Ra_x}{Pe_x})(\theta' + N\varphi') + 2\Lambda F''F'$ (15)

Let $A[i] = (1+Ha^2+2\Lambda F')$,

$B[i] = (2\Lambda F'')$ and

$D[i] = \mp(\frac{Ra_x}{Pe_x})(\theta' + N\varphi') + 2\Lambda F''F'$

Then equation (15) can be written as

$A[i]\,f'' + B[i]\,f' = D[i]$ (16)

Where F is known function, which is the value of f at (n-1)th iteration and f is unknown function at nth iteration. To solve the system of equation , we apply the implicit finite difference scheme to equation (16) ,(10) and (11) . We get

$$\begin{aligned} &a[i]f[i-1] + b[i]f[i] + c[i]f[i+1] = d[i] \\ &a1[i]\theta[i-1] + b1[i]\theta[i] + c1[i]\theta[i+1] = d1[i] \\ &a2[i]\varphi[i-1] + b2[i]\varphi[i] + c2[i]\varphi[i+1] = d2[i] \end{aligned} \quad (17)$$

where

$a[i] = A[i] - hB[i]/2$, $b[i] = -2A[i]$, $c[i] = A[i] + hB[i]/2$ and $d[i] = h^2 D[i]$.
$a1[i] = 1 - hB1[i]/2$, $b1[i] = -2$, $c[i] = 1 + hB1[i]/2$ and $d1[i] = h^2 D1[i]$.
$a2[i] = A2[i] - hB2[i]/2$, $b2[i] = -2A2[i] + h^2 C2[i]$, $c2[i] = A2[i] + hB2[i]/2$
$B1[i] = f[i]/2$ and $D1[i] = -Pr\ Ec\ (f'')^2$

$A2[i] = 1/Sc$, $B2[i] = -\tau\theta'[i] + \frac{1}{2Pr} f[i]$ and $C2[i] = -\tau\varphi'[i]$

Here the step size taken as h=0.2 is obtain the numerical solution with η_{max} =6 and solved the algebraic system equations by using Gauss-sidel method and five decimal accuracy as the criterion for convergence.

RESULTS AND DISCUSSION

For the present problem numerical computations are carried out for different flow parameters such as inertia parameter Λ, Thermal Rayleigh number Ra_x , local polet number Pe_x, buoyance ratio N, Schmidt number Sc ,thermophoretic parameter τ , Eckert number Ec and Magnetic parameter Ha. In addition the boundary condition $\eta \rightarrow \infty$ is approximated by $\eta_{max}=6$; which is sufficiently large for the velocity to approach the relevant stream velocity.

Figures 1-6 represent typical velocity profiles for various values of different flow parameters. Fig.1 demonstrates the effect of thermophoretic parameter τ. It is observed that an increasing of thermophoretic parameter τ leads to a decreasing in the velocity profiles. The effect of mixed convection parameter Ra_x/Pe_x on the velocity profile is shown in fig.2 and it is observed that the velocity profile increases with the increasing of mixed convection parameter Ra_x/Pe_x. Fig.3 shows that the variation in velocity profiles due to change in Schmidt number Sc , the Schmidt number Sc values are chosen as Sc =0.2(Hydrogen), Sc=0.6(water weeper), Sc=0.78(Ammonia), which represents diffusing chemical species of most common interest in air at 20°C and one atmosphere pressure. The velocity profiles decreases with the increase of Sc. The velocity profiles increases with the increase of buoynce parameter N and inertia parameter Λ is noticed from the fig. 4. The influence of viscous dispersion effect on velocity profiles is shown in fig.5. An increase in the viscous dispersion parameter results in an increasing of the velocity profiles is observed. Fig.6 illustrates the influence of magnetic parameter Ha on the velocity profiles. It is observed that an increase the magnetic parameter Ha, decreases the Hydro magnetic boundary layer causing the reduced the fluid velocity.

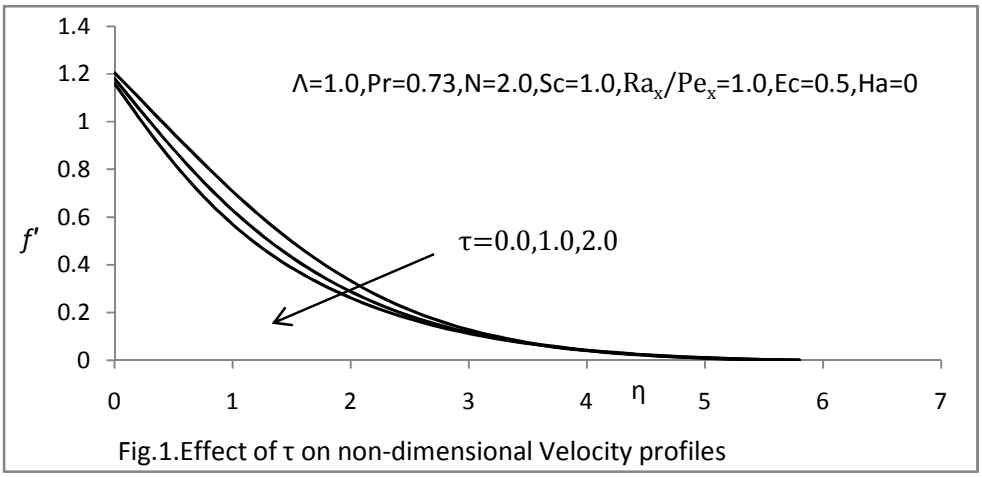

Fig.1.Effect of τ on non-dimensional Velocity profiles

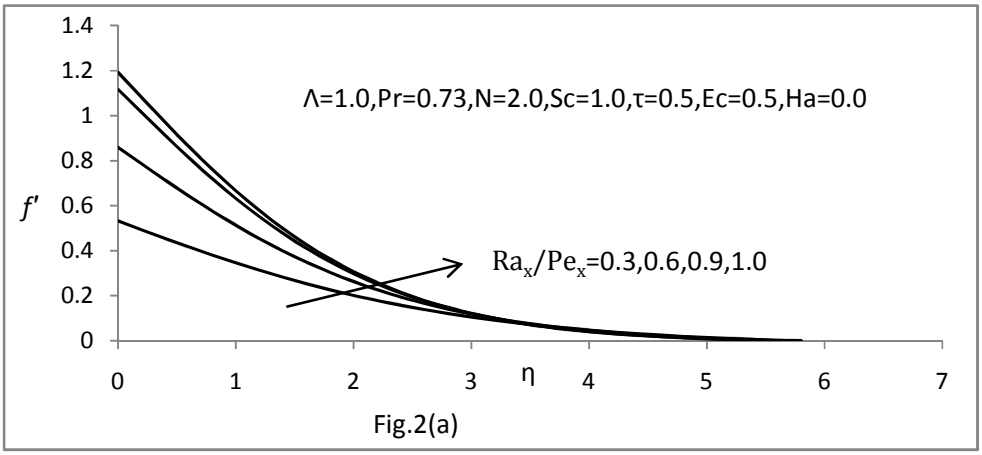

Fig.2(a)

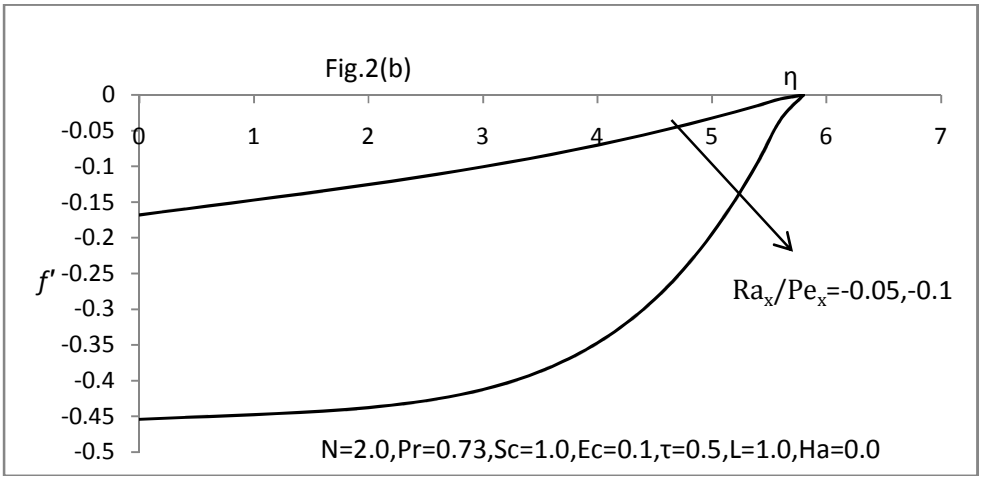

Fig. 2(a)&(b).Effect of Ra_x/Pe_x on non-dimensional velocity profiles.

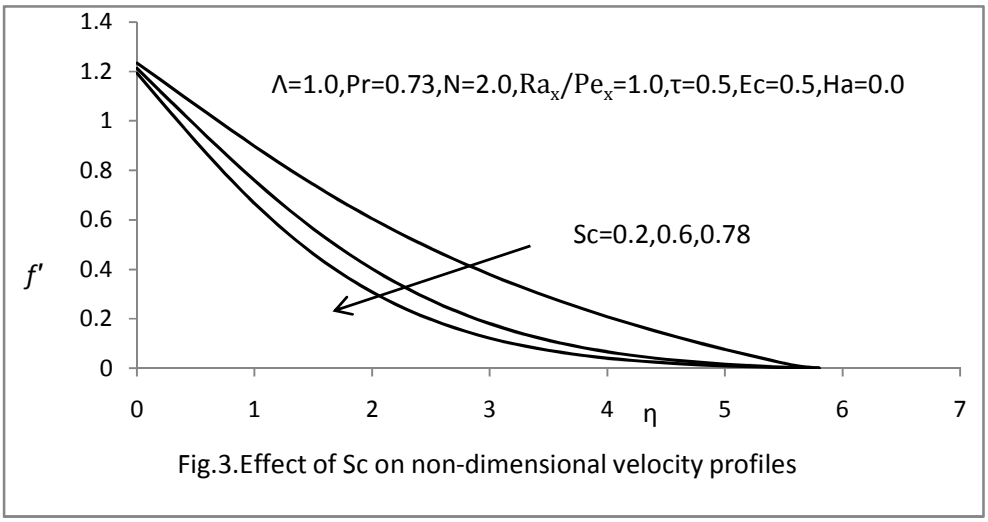

Fig.3.Effect of Sc on non-dimensional velocity profiles

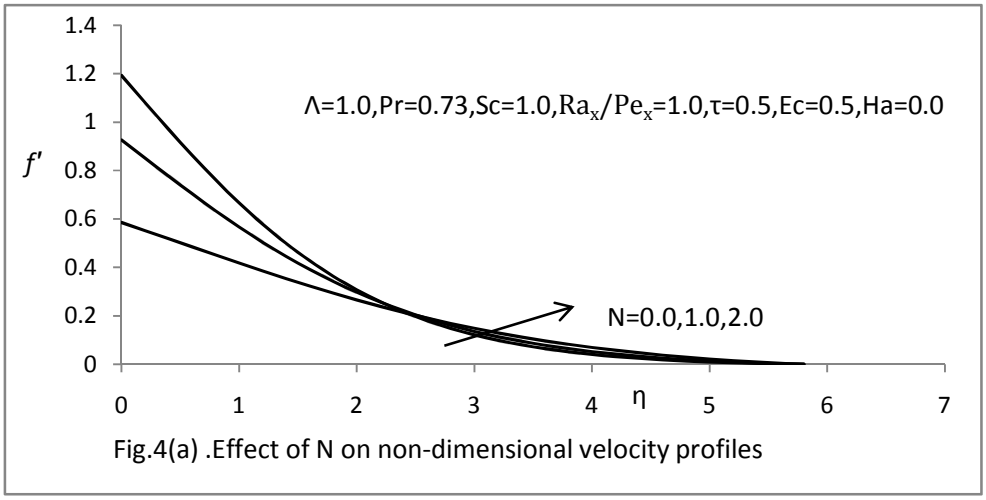

Fig.4(a) .Effect of N on non-dimensional velocity profiles

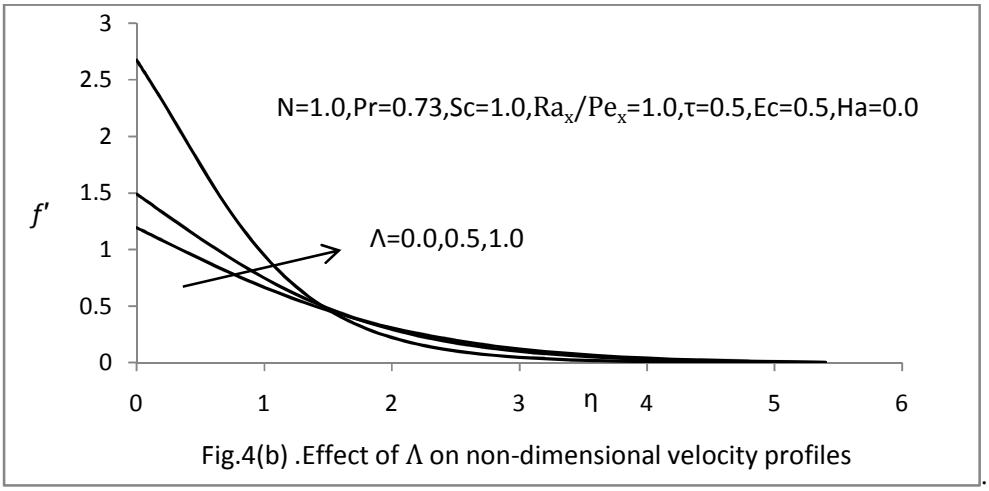

Fig.4(b) .Effect of Λ on non-dimensional velocity profiles

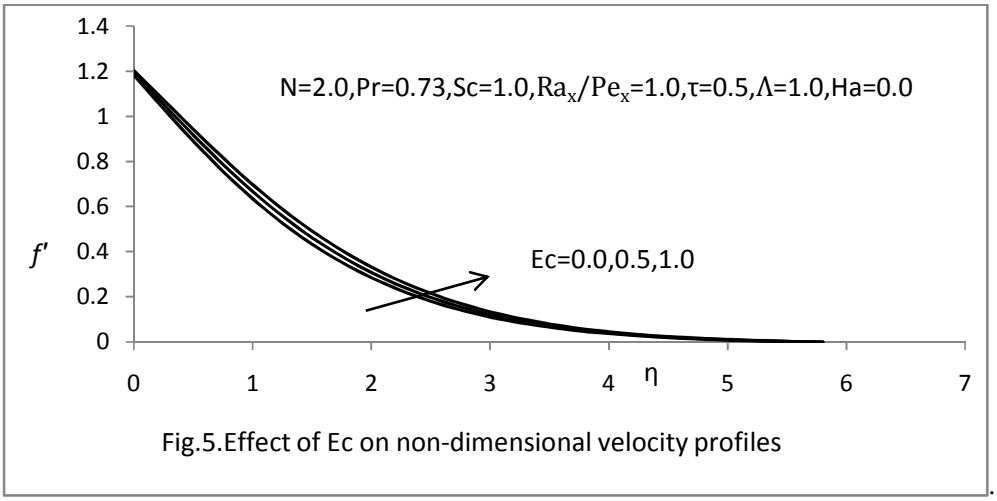

Fig.5.Effect of Ec on non-dimensional velocity profiles

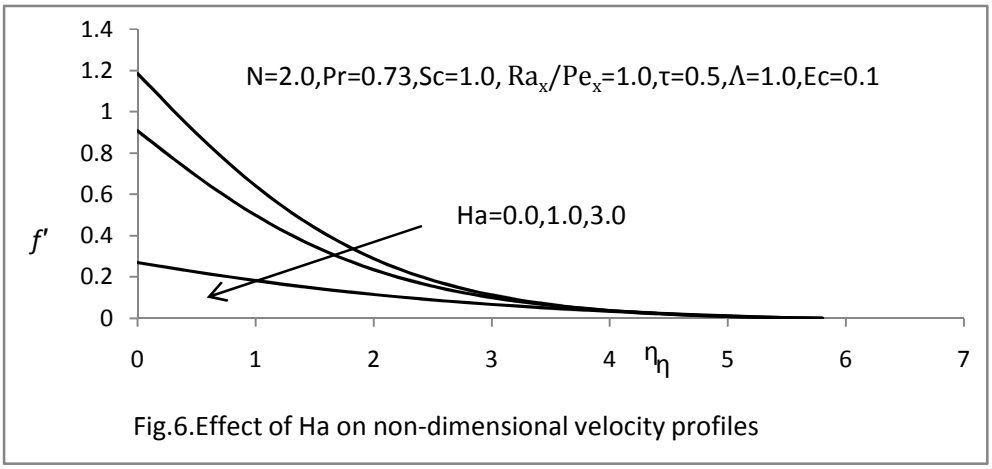

Fig.6.Effect of Ha on non-dimensional velocity profiles

Figures 7-12 show that the effects of various parameters on temperature profiles. The influence of thermophoretic parameter τ on temperature profiles is shown in fig.7. It is noticed from the figure that increasing thermophoretic

parameter τ leads to slidely increase fluid temperature. The effect of mixed convection parameter Ra_x/Pe_x is shown fig.8.

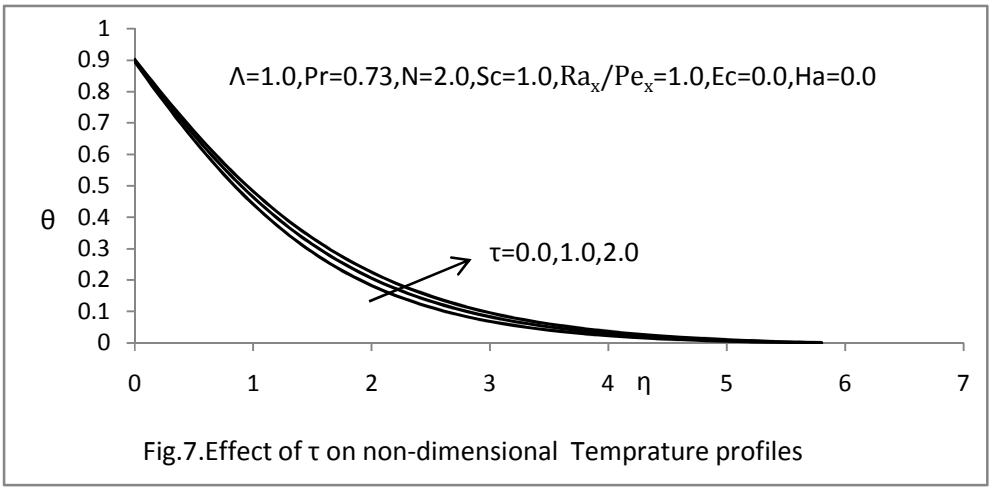

Fig.7.Effect of τ on non-dimensional Temprature profiles

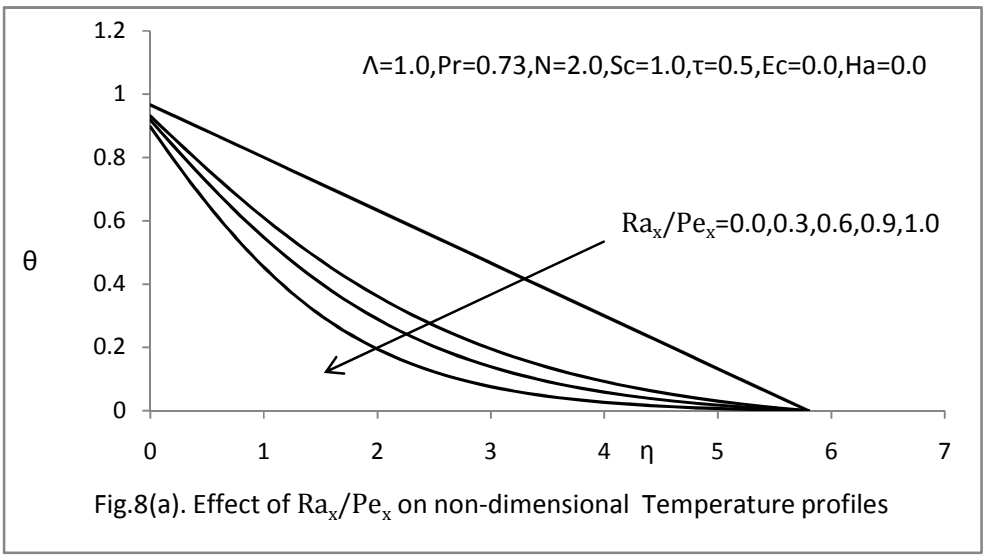

Fig.8(a). Effect of Ra_x/Pe_x on non-dimensional Temperature profiles

The temperature profile decreases with the increase of Ra_x/Pe_x is noticed. A rise in the Schmidt number Sc from 0.2 – 0.78 leads to increases in temperature profiles is observed from fig.9. The temperature profiles is drawn the for different values on buoynce parameter N in fig.10 .The effect of byounce ratio parameter N is leads to decrease the temperature profiles . The effect of inertia parameter Λ on the temperature profiles in the present and absence of the viscous dispersion effect is shown in fig.11 . It is observed that an increase in the inertia parameter Λ is leads to increase in the fluid temperature, in absence of viscous dispersion; where as with effect of inertia parameter Λ leads to increase with the temperature profiles near the boundary and reverse phenomenon is observed far away from the boundary. The viscous dispersion and magnetic parameter effects on temperature profiles is shown in fig.12. With the effect of viscous dispersion and Maganetic parameter Ha there is a significant increase in the temperature profiles is noticed.

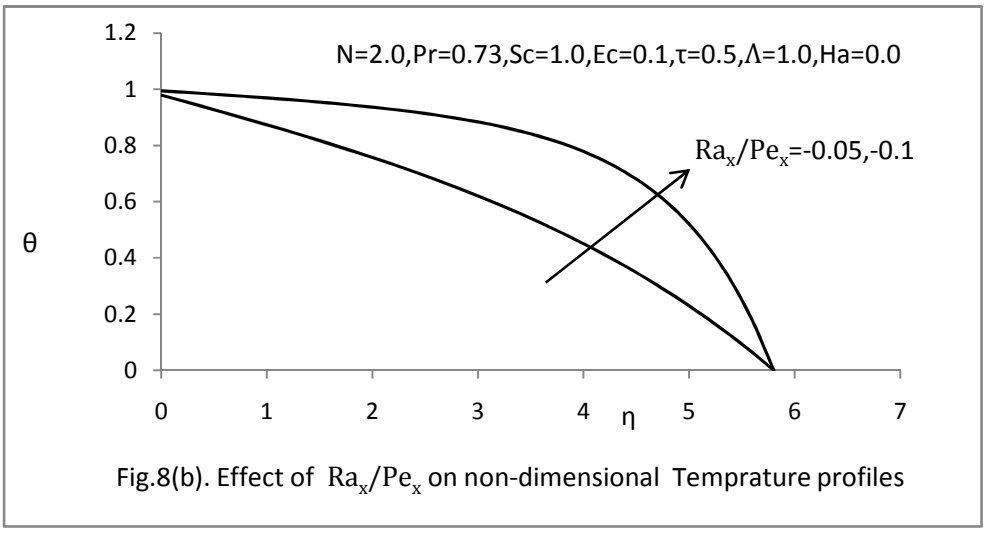

Fig.8(b). Effect of Ra_x/Pe_x on non-dimensional Temprature profiles

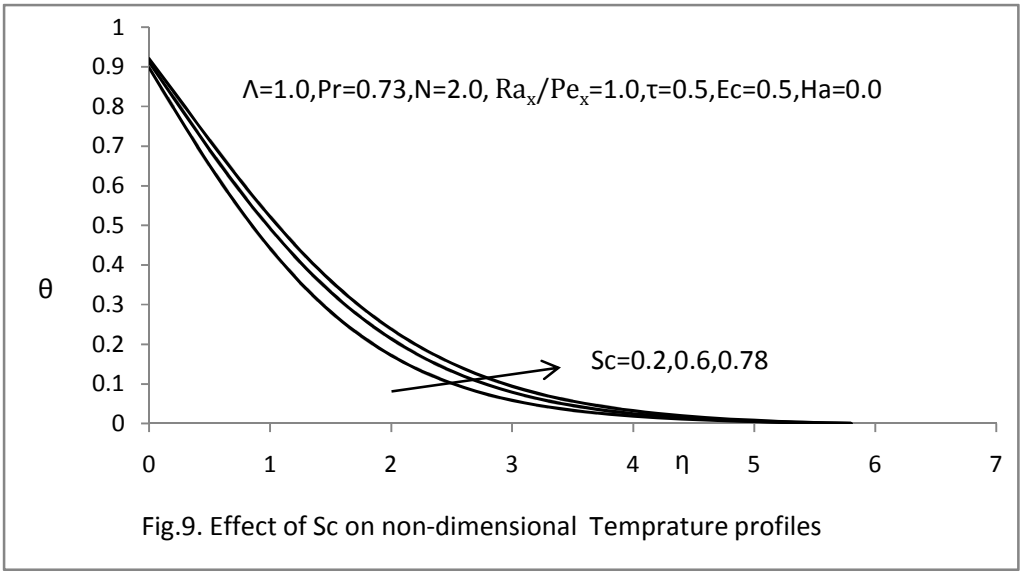

Fig.9. Effect of Sc on non-dimensional Temprature profiles

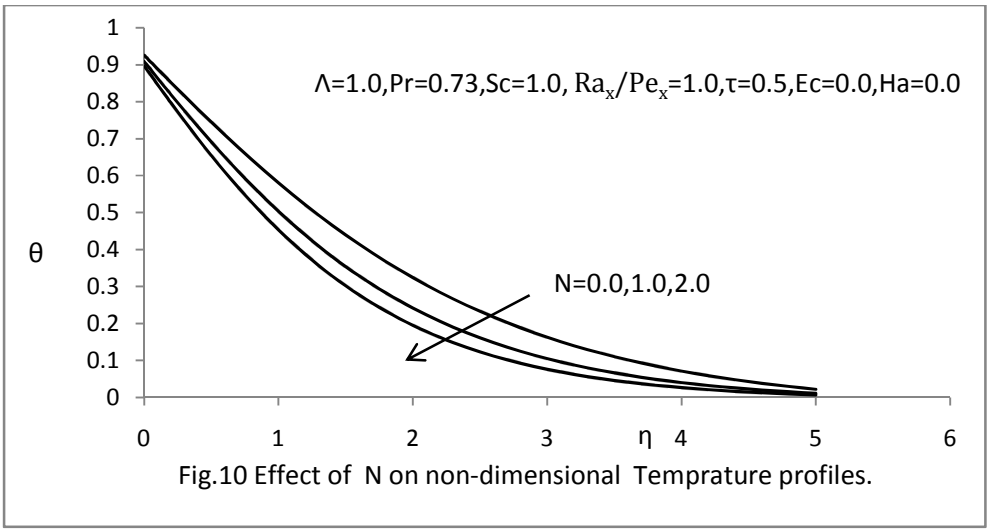

Fig.10 Effect of N on non-dimensional Temprature profiles.

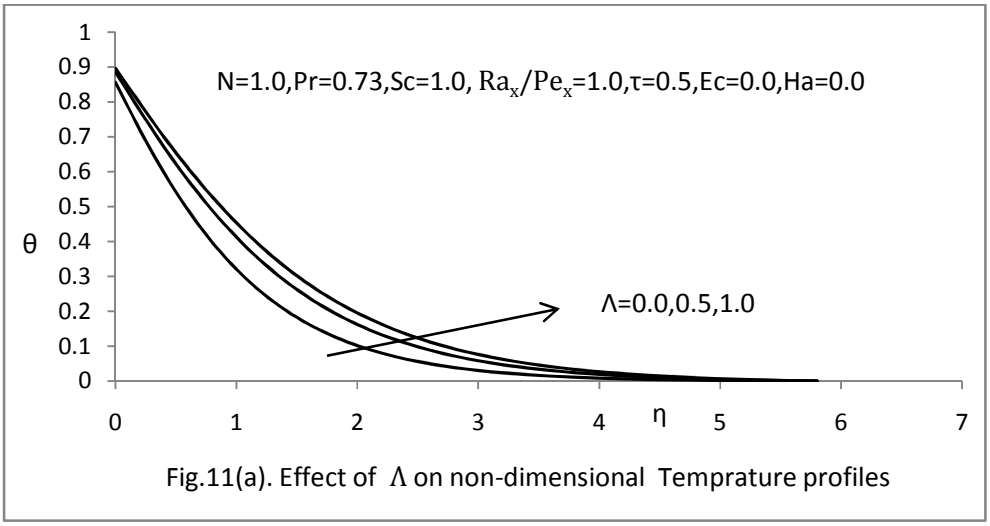

Fig.11(a). Effect of Λ on non-dimensional Temprature profiles

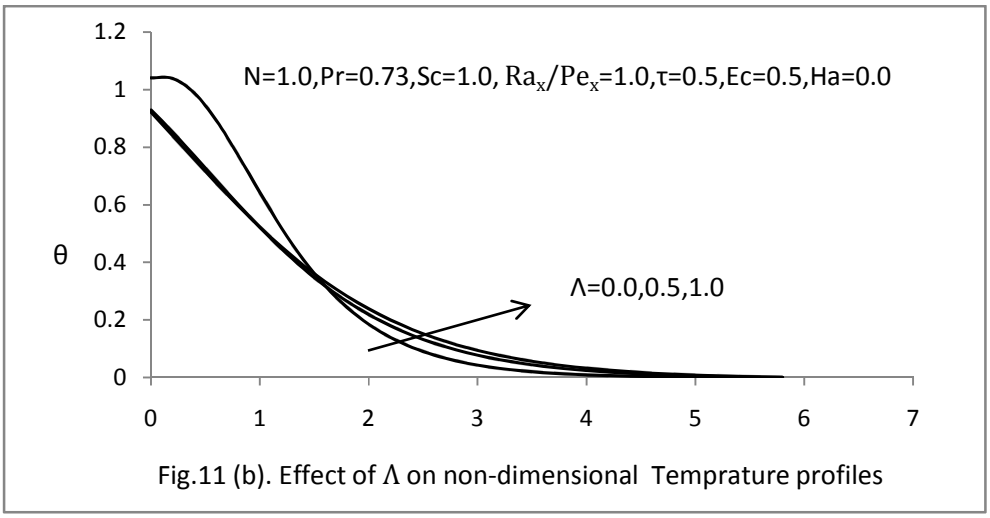

Fig.11 (b). Effect of Λ on non-dimensional Temprature profiles

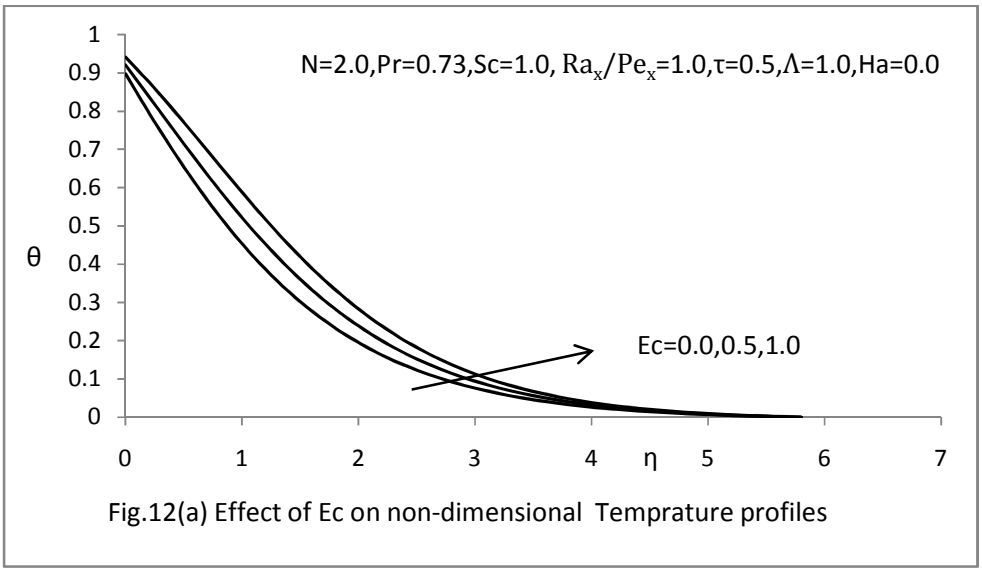

Fig.12(a) Effect of Ec on non-dimensional Temprature profiles

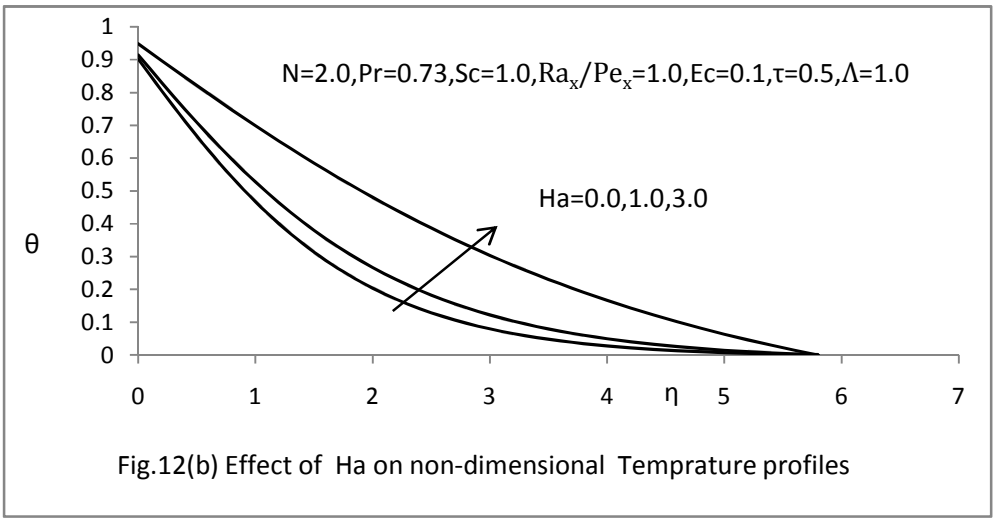

Fig.12(b) Effect of Ha on non-dimensional Temprature profiles

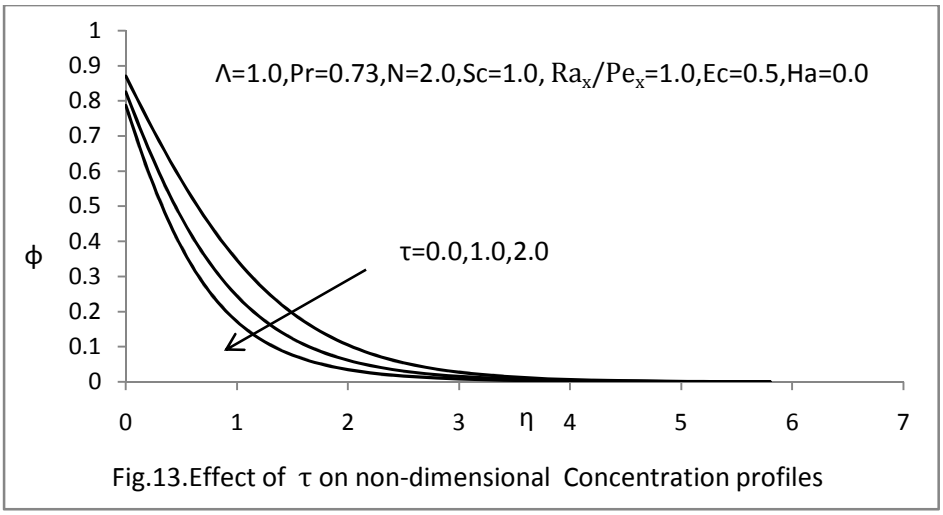

Fig.13.Effect of τ on non-dimensional Concentration profiles

Figures 13-19 represent typical concentration profiles for various values of different flow parameters. Fig .13 depict the effect of thermophoretic parameter τ on the concentration profiles .The effect of thermophoretic parameter τ is to reduces the concentration profiles is observed. From the fig.14 it is noticed that the effect of mixed convection parameter Ra_x/Pe_x is to increases the concentration profiles . The infience of Schmidt number Sc is shown in figure 15 and the influence of buoynce parameter N is represented in fig 16. From these figures the effect of Schmidt number Sc and buoynce parameter N is decelerates the concentration profiles. Fig.17 illustrates the effect of inertia parameter Λ on concentration profiles, it is observed that the concentration profiles increases with increase of inertia parameter Λ. The influence of magnetic parameter Ha on concentration profiles displayed in fig.18. The magnetic field effect is to accelerates the concentration profiles. The influence of viscous dissipation effect on concentration profiles is shown in fig.19. As shown from the figure the effect of viscous dissipation is negligible in concentration profiles. The heat and mass transfer results in terms of $Nu_x/Pe_x^{1/2}$ and $Sh_x/Pe_x^{1/2}$ as functions of the mixed convection parameter Ra_x/Pe_x with and without viscous dissipation effect at different values of thermophoretic parameter are displayed in figures 20 and 21. While τ increasing $Nu_x/Pe_x^{1/2}$ decreasing and $Sh_x/Pe_x^{1/2}$ increasing in the presence and absence Ec. It is worth pointing out that at Ec ≠ 0, the effect of τ on $Nu_x/Pe_x^{1/2}$ is more than in the case of Ec = 0 and the opposing phenomena occurs with $Sh_x/Pe_x^{1/2}$. Also, as Ec increases, $Nu_x/Pe_x^{1/2}$and $Sh_x/Pe_x^{1/2}$decrease greatly. On the other hand, when Ra_x/Pe_x increases $Nu_x/Pe_x^{1/2}$and $Sh_x/Pe_x^{1/2}$decrease in the presence of Ec, but it increases in the absence of Ec, as shown in figures 20 and 21. This is

because increasing Ra_x /Pe_x increases the momentum transport in the boundary layer and more heat and mass species are carried out of the surface, thus decreasing the thickness of the thermal and concentration boundary layer and hence increasing the heat and mass transfer rates.

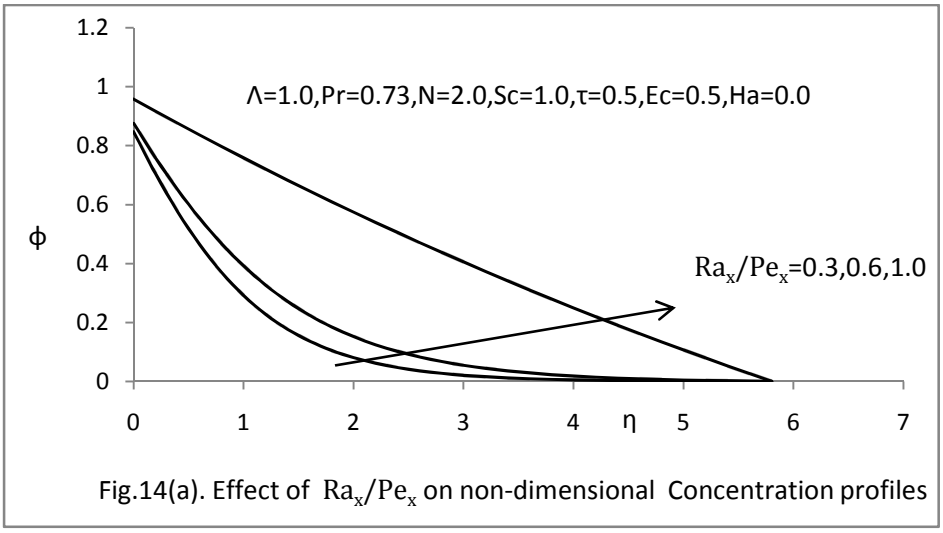

Fig.14(a). Effect of Ra_x/Pe_x on non-dimensional Concentration profiles

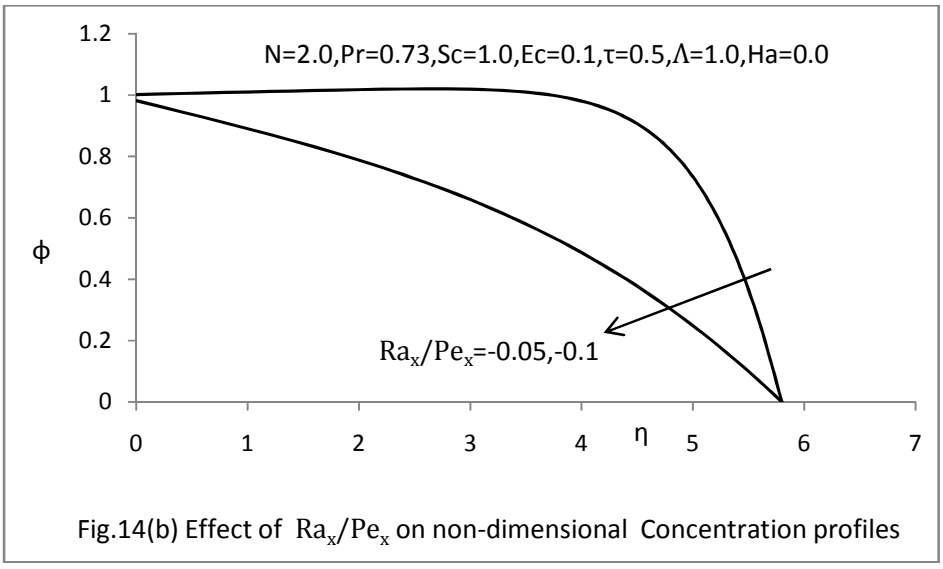

Fig.14(b) Effect of Ra_x/Pe_x on non-dimensional Concentration profiles

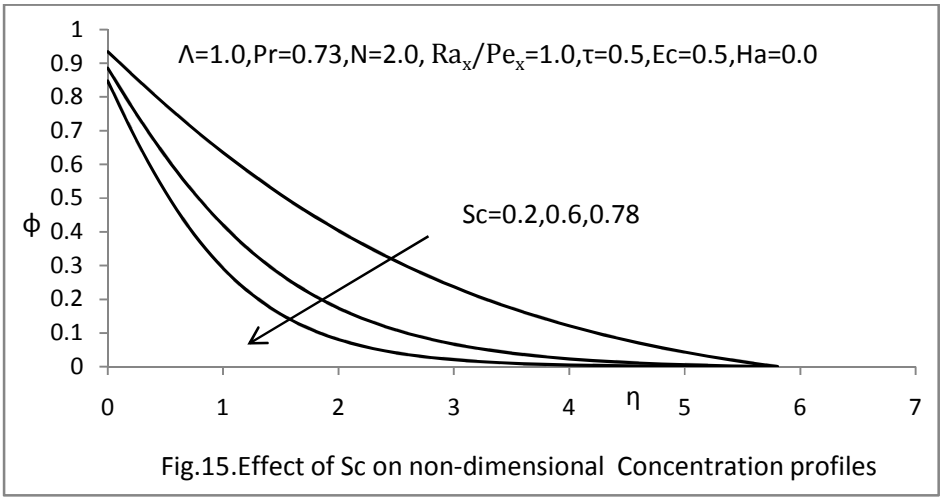

Fig.15.Effect of Sc on non-dimensional Concentration profiles

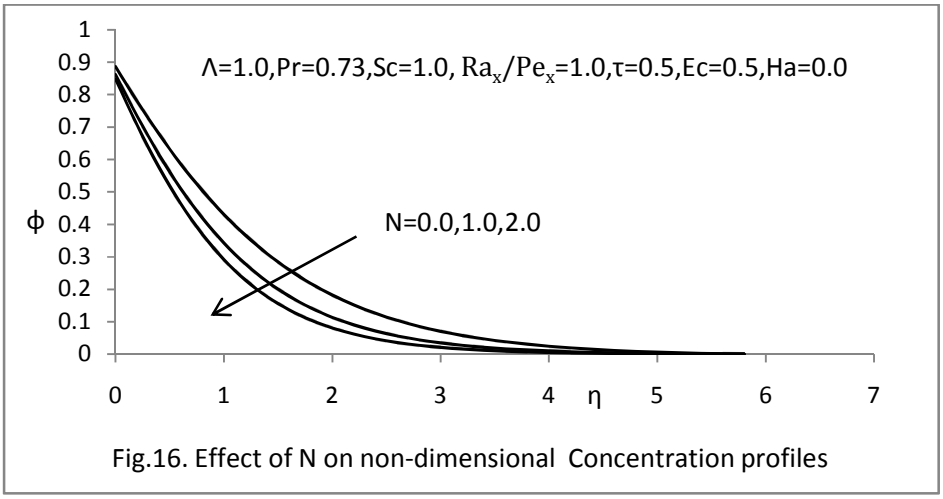

Fig.16. Effect of N on non-dimensional Concentration profiles

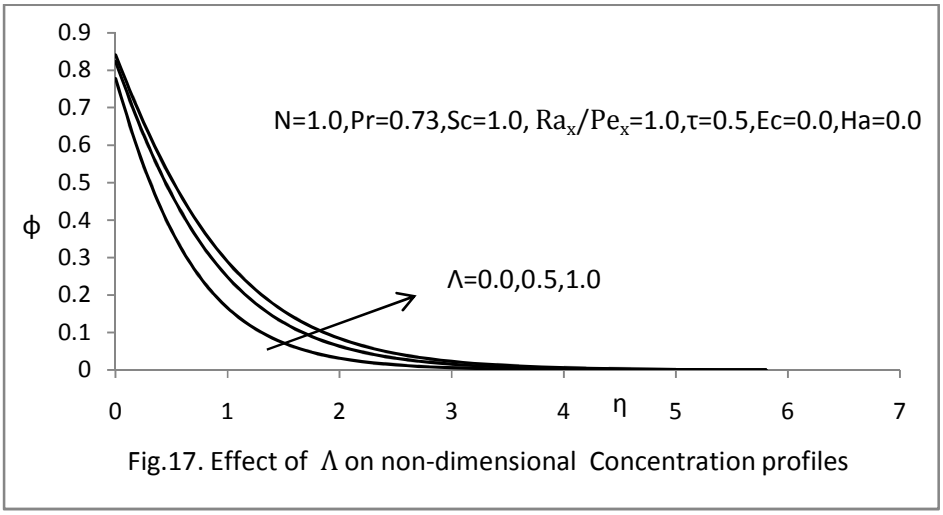

Fig.17. Effect of Λ on non-dimensional Concentration profiles

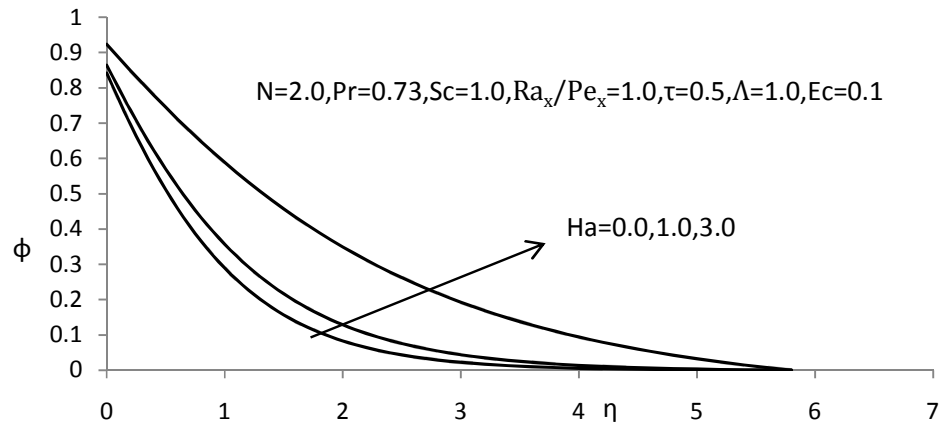

Fig.18. Effect of Ha on non-dimensional Concentration profiles

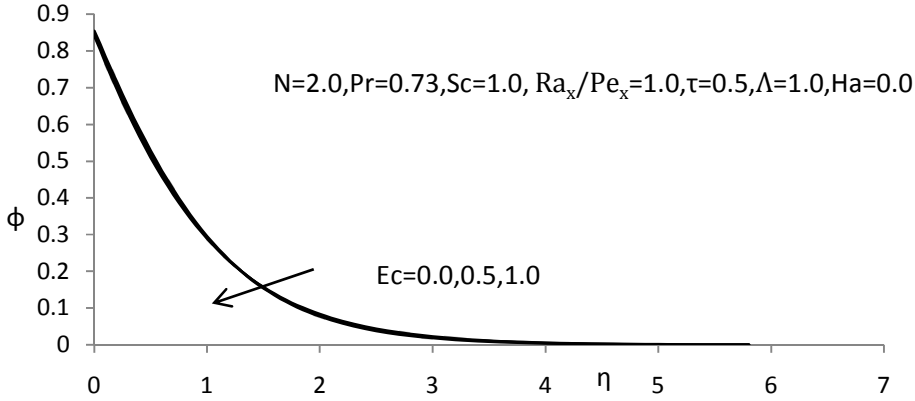

Fig.19.Effect of Ec on non-dimensional Concentration profiles

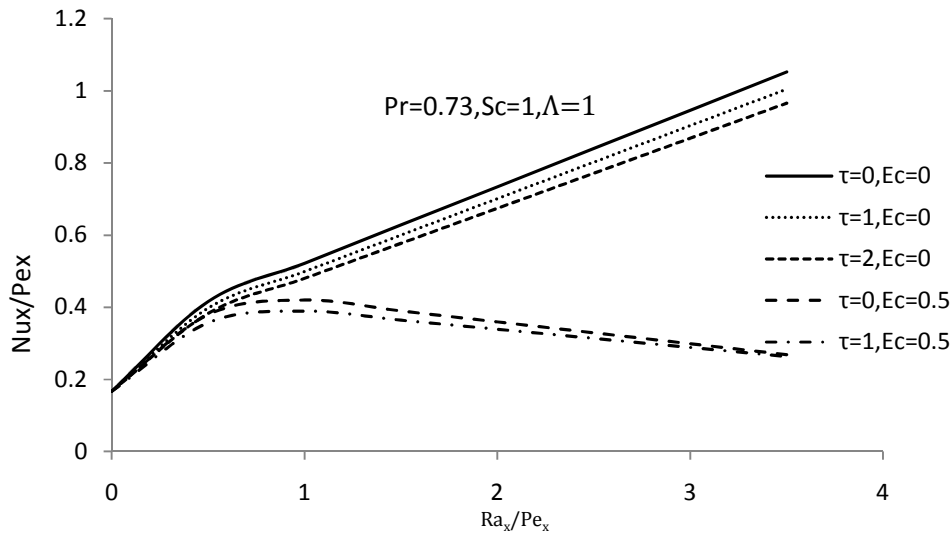

20.Local Nusselt number as a function of Ra$_x$/Pe$_x$for various values of τ and Ec

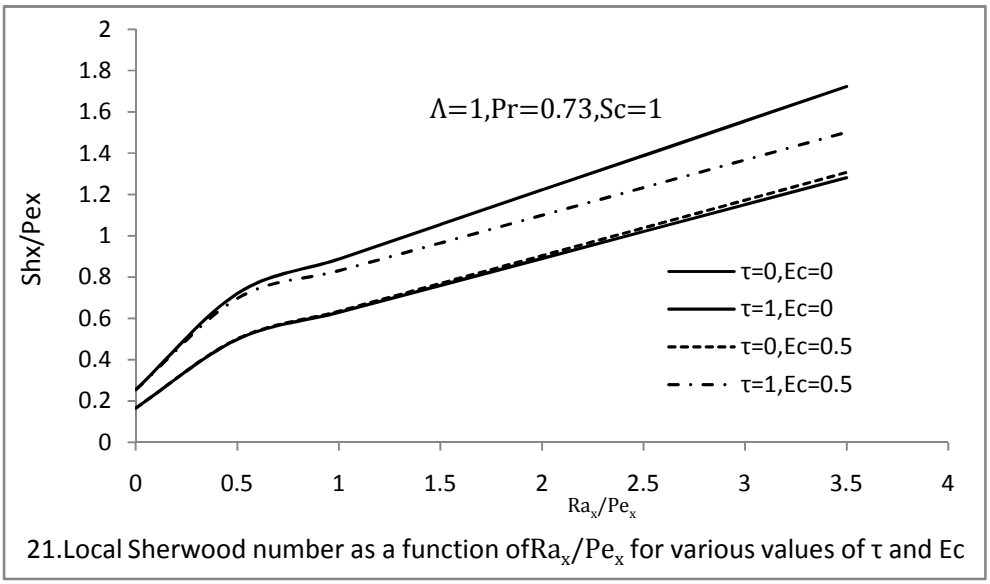

21.Local Sherwood number as a function ofRa_x/Pe_x for various values of τ and Ec

REFERENCES

[1] D.A. Nield, *Water Resour. Res*. 4 (**1968**) 553–560.
[2] A. Bejan, K.R. Khair, *Int. J. Heat Mass Transfer* 29 (**1985**) 909–918.
[3] A. Yucel, *Int. J. Heat Mass Transfer* 33 (**1990**) 2265–2274.
[4] F.C. Lai, F.A. Kulaki, *ASME J. Heat Transfer* 34 (**1991**) 887–990.
[5] Kremer, D.M., Davis, R.W., Moore, E.F., et al.: *J. Electrochemical Society* **150**(2), 918-922 (**2003**)
[6] Y.J. Rami, A. Fawzi, F. Abu-Al-Rub, *Int. J. Numer. Methods Heat Fluid Flow* 11(**2001**) 600-618.
[7] S.L. Goren, *J. Colloid Interface Sci*. 61 (**1977**) 77.
[8] Y.P. Chang, R. Tsai, F.M. Sui, *J. Aerosol Sci*. 30 (**1999**) 1363–1378.
[9] S. Jayaraj, K.K. Dinesh, K.L. Pillai, *Heat Mass Transfer* 34 (**1999**) 469–475.
[10] R. Tsai, Int. Commun. *Heat Mass Transfer* 26 (**1999**) 249–257.
[11] A. Selim, M.A. Hossain, D.A.S. Ress, *Int. J. Thermal Sci*. 42 (**2003**) 973–982.
[12] A.J. Chamkha, I. Pop, *Int. Commun. Heat Mass Transfer* 31 (**2004**) 421–430.
[13] G. Peev, A. Nikolova, D. Todorova, *Chem. Eng. J*. 88 (**2002**) 119–125.
[14] B. Gebhart, *J. Fluid Mech.* 14 (**1962**) 225.
[15] L. Talbot, R.K. Cheng, R.W. Scheffer, D.P. Wills, *J. Fluid Mech*. 101(**1980**) 737–758.
[16] G.K. Batchelor, C. Shen, *J. Colloid Interface Sci*. 107 (**1985**) 21–37.
[17] Talbot, L., Cheng, R.K., Schefer, R.W., et al.: *J. Fluid Mech.* **101**(4),737–758 (**1980**)
[18] Kanki, T., Luchi, S., Miyazaki, T., et al.: *J.Colloid. Interf. Sci*. **107**(2), 418–425 (**1985**)
[19] M.A.Seddek, et al: *Journal of Colloid and interface Science* 293 (**2006**) 137-142.
[20] M. K. Partha, et al : *Heat Mass Transfer* (**2008**) 44:969–977.
[21] Joaqu´ın Zueco , O. Anwar B´eg , L.M. L´opez-Ochoa, *Acta Mech. Sin*. (**2011**) 27(3):389–398.
[22]Ismoen Muhaimin , Ramasamy Kandasamy & Ishak Hashim ; *International Journal for Computational Methods in Engineering Science and Mechanics*, 10:231–240, **2009**.
[23]N.P. Singh , Ajay Kumar Singh , Atul Kumar Singh , Pratibha Agnihotri, *Commun Nonlinear Sci Numer Simulat* 16 (**2011**) 2519–2534.
[24] Bellman R.E. and Kalaba R.E, **1965**. Quasi-Linearization and Non-linear boundary value problems, Elsevier, New York.